



Case Studies

Slug Flow Control in an S-shape Pipeline-Riser System using an Ultrasonic Sensor

Somtochukwu Godfrey Nnabuife^a, Henry Tandoh^a, James Whidborne^{c,*}^a Geo-Energy Engineering Centre, Cranfield University, Cranfield, MK43 0AL, United Kingdom^c Dynamics Simulation and Control Group, Cranfield University, Cranfield, MK43 0AL, United Kingdom

ARTICLE INFO

Keywords:

Doppler ultrasound
Slug flow
S-shaped riser
Multiphase flow
Riserbase pressure

ABSTRACT

Slugging flow poses significant challenges to the offshore multiphase flowline and riser systems. Slug flow is characterized by an uneven flow regime whereby pipeline pressures, temperatures, or flow volume rates fluctuate. One of the most common causes of severe slugging is low pressures which causes buildup of fluid over time, consequentially causes flow and pressure oscillations. This mostly occurs in vertical risers or wells. The negative effects of severe slugging have prompted numerous studies, investments, and efforts to reduce or eliminate the slugging flow. Several active slugging control techniques have been investigated in the oil and gas industries for decades. However, many of these techniques still run the risk of limiting hydrocarbon production due to inappropriate over choking. Other challenges for active slug control include the fact that some systems rely mainly on subsea measurements such as riser base pressure, and most of these subsea measurements are costly, difficult to maintain, not always available, and can be unreliable. As a result, to achieve an efficient slugging control performance, reliable, robust, and efficient measurements that are more sensitive to slugging flow for control are required, which is the motivation for this work. The control of riser slug flow using non-radioactive, non-invasive, and non-intrusive Continuous-wave Doppler ultrasound has been investigated in this work, and provides good control performance. It achieved a larger valve opening than an open-loop unstable system. This outperforms manual choking, which maintains stability at a much lower valve opening.

1. Introduction

Offshore oil and gas production and exploration facility production optimization has received a lot of attention in recent years, since any prospective increased hydrocarbon recovery can result in substantial economic advantages. As a result, multiphase flow behaviour in pipeline-flowlines, for which slugging flow belongs, is a major problem in the offshore oil and gas sectors. A significant amount of time and money has been spent researching the slugging phenomenon. The reason for this is that any change in operating conditions has the potential to significantly alter pipeline flow behaviour. This has a substantial influence on key aspects like safety, maintenance, and production (Havre et al., 2000).

Due to pressure and flow rate variations in the system, an undesired flow regime occurs under certain operating circumstances, which may cause serious difficulties at topside processing facilities. This usually happens at the end of a well's life, when the flow rates in the system are significantly lower than what the system was intended for. A flow

regime known as slugging flow causes these pressure and flow rate variations (Payne et al., 1996, Cao, 2011).

Slugging flow has a detrimental impact on topside processing facilities during offshore oil and gas production. Slugging is known to produce a reduction in operational capacity as well as undesired flaring. Variations in pressure can put a strain on some elements of the system, such as bends and valves. In most situations, the burden of the topside compressors and separators becomes so great that it causes extensive damage and plant closure, which is a major disadvantage for oil-producing companies (Taitel et al., 1990).

Avoiding slugging flow in the pipeline results in significant economic advantages. As a result, it is critical to forecast or identify the flow regime before beginning production to address problems as soon as feasible. Flow regime maps are typically created to forecast the flow regime that will occur in the pipeline (Hewitt and Roberts, 1969, Taitel, 1986, Barnea, 1987). The flow regime is approximated using the following quantities: gas/liquid densities, pipe diameter, gas/liquid viscosities, gas/liquid surface tension, pipe inclination, and gas/liquid superficial velocities (Griffith, 1961). Because these quantities can change throughout the pipeline, so can the flow regime. The flow regime map is de-

* Corresponding author: Dr James Whidborne, Cranfield University, Dynamics Simulation and Control Group, Cranfield MK43 0AL, United Kingdom, Phone: +447500004602

E-mail address: j.f.whidborne@cranfield.ac.uk (J. Whidborne).

<https://doi.org/10.1016/j.dche.2021.100005>

Received 15 September 2021; Received in revised form 24 November 2021; Accepted 6 December 2021

2772-5081/© 2021 The Author(s). Published by Elsevier Ltd on behalf of Institution of Chemical Engineers (IChemE). This is an open access article under the CC BY-NC-ND license (<http://creativecommons.org/licenses/by-nc-nd/4.0/>)

scribed by the flow regime's dependency on the aforementioned factors (Hewitt and Roberts, 1969).

Slugging flow prevention or control has significant economic benefits, which is why a great deal of time and money has been invested in the quest for a solid solution to the issues created by slugging flow. Slugging can be prevented or controlled by a variety of methods, including design modifications. For example, expanding the size of the separators, installing a gas lift or slug catcher, or altering the pipeline topology. As a result, the installation and management of this new technology is costly. The next technique is to change the system operating conditions by restricting the topside valve. As a result, the main downside of this approach is a decrease in production rate owing to increased pressure in the pipeline (Pedersen et al., 2017).

Much research has been conducted over the last few decades on the use of active control as a technique for flow stabilisation. Schmidt et al (Schmidt et al., 1979) successfully built an automated control system on a pipeline-riser system using a topside choke valve as an actuator. Hedne and Linga (Pal and Harald, 1990) demonstrated that by using a PI controller and a pressure sensor to estimate the difference in pressure above the riser, it is feasible to stabilise the flow. Recently, several control approaches have been successfully applied to an offshore production system (Havre et al., 2000, Courbot, 1996, Godhavn et al., 2005).

The active control system modifies the flow regime map's borders, preventing slugging in areas where the slug was expected. Thus, it is possible to maintain the same average flow rate as previously without experiencing large variations in pressure and flow rates.

The advantages of using active control are enormous. It is more cost-effective and efficient than deploying new equipment, and it may efficiently minimise large liquid surge movement in the system, reducing strain on the system. As a result, system maintenance difficulties will be decreased, and a significant amount of money will be saved. Furthermore, active control allows for higher output rates than traditional choking of the topside valve.

Pressure measurements at the riser base or farther upstream are some of the measures that have been used during subsea multiphase measurements. Subsea measurements have been shown to be useful in slugging mitigation/control. As a result, in the absence of these metrics, slug mitigation/control becomes more difficult (Taitel et al., 1990). Subsea measurements are frequently unavailable, costly to implement, and less accurate than topside data. It is critical to determine the potential of slug control using just topside measurements, therefore the birth of topside measurements. However, several issues were raised, such as the possibility of enhancing system performance by utilising a single topside measurement or a mixture of topside information; are these findings the same or equivalent to those obtained when a controller based on subsea measurements was deployed. To answer these issues, novel multiphase flow topside measurements that will provide acceptable control performance are being explored. Some of the work on slug flow control using topside measurements can be found in (Nnabuife et al., 2021), which includes the Inferential Slug Control (ISC) (Cao et al., 2013). The ISC system detects the production of slugs inside a pipeline or riser using numerous accessible measurements on a platform and actively operates a control valve to attenuate the slug before it enters a sensitive area of the process system in real time. It is envisaged that by installing such a device, slug flow fluctuations would be reduced, leading to the reliable and safe operation of offshore production systems. Because of the lower average pipeline pressure after slugging is attenuated, an instantaneous boost in output may be realised. Separators and other equipment will be shielded from the slug's harmful kinematic effects. The ISC system also employed the use of gamma signals, which are radioactive in nature.

The ability to describe the characteristics of multiphase flows utilising non-radioactive, non-invasive, quick reaction, and suited for opaque systems has sparked the interest of numerous industrial applications. As a result, ultrasonic methods credibly satisfy all of these requirements. When compared to conventional techniques such as X-ray and Gamma-ray, there are several benefits to using ultrasonic techniques measure-

ments such as speed, high precision, greater sensitivity, safety, and ease of deployment (Zhai et al., 2013, Nnabuife et al., 2020).

The standard ultrasonic pulse-wave Doppler (PW) has been used in medicine since 1986. The main disadvantage of PW is its inability to measure maximum velocity (Zhai et al., 2013). The PW Doppler ultrasonography can only measure velocities unambiguously up to a maximum limit linked to the depth of examination. The highest Doppler frequency shift that a PW Doppler device can detect is half the pulse repetition frequency (PRF). When a result, as the depth of the examined region increases, the PRF must be decreased to provide the pulses adequate time for another round trip. As a result, lesser velocities can be observed in deeper channels (Takeda, 1999). The difficulty of maximum velocity measurement is more significant when measurements on high-velocity flow regimes, such as slug flow, are required.

The suitability of Continuous-Wave Doppler methods for slug flow control was explored in this paper. The CW Doppler has no upper limit on the highest velocity it can measure. Because of the low sample rates used in PW Doppler, this is not the case. To estimate or extract Doppler shift from an ultrasound signal, the velocimeter analyses the phase connection between each continuous returning pulse ultrasound and a signal from the reference oscillator. Because angular measurements repeat themselves every 2π radians, the greatest phase change that may be seen on each side of the two pulses is limited to a range of $-\pi$ to $+\pi$ radians. As a result, if the target travels more than $\lambda/4$ times the distance between the samples, its velocity may be misinterpreted. This disadvantage stems from the sampling theorem statement, which stipulates that to avoid ambiguity, a signal must be sampled at least twice its maximum frequency (Atkinson and Wells, 1977, Okamura et al., 1989).

The following are the main contributions of this paper: (i) this paper demonstrated the use of ultrasonic signals in the Inferential Slug Controller (ISC) for slug flow control, which will also improve ISC functionality; and (ii) this is the first known attempt to use Continuous Wave Doppler Ultrasound (CWDU) for slug flow control in an S-shaped riser. This paper is organised as follows: Section 2 discusses the ultrasonic sensor and algorithm utilised in this research, Section 3 covers the experimental setup, Section 4 shows the data obtained, and Section 5 summarises this work.

2. Measurement Sensor and Algorithm

2.1. Continuous Wave Ultrasonic Doppler

Doppler Effect (Doppler shift) is the frequency fluctuation of an acoustic wave that occurs when there is movement between the acoustic receiver and the source, and the frequency shift is proportional to the acoustic source velocity (Weinstein, 1982). Thus, computing the frequency shift between the acoustic receiver and the source yields the velocity of the acoustic source. A fixed frequency acoustic beam is constantly discharged from the transducer (ultrasonic) into the flow in the ultrasonic Doppler method, and the sound wave is reflected by moving the scatters [(Nnabuife et al., 2020). The dispersed acoustic beam is received by another ultrasonic transducer, and the flow velocity is calculated using the frequency shift based on the Doppler Effect (Nnabuife et al., 2019).

The outline of the instrumentation process needed to detect shifts in Doppler of the received ultrasound Figure 1 and described below: Assuming the signal transmitted is

$$x_t(t) = \epsilon_t \cos(\omega_s t) \quad (2.1)$$

and the corresponding received signal from one of the scatters is

$$x_r(t) = \epsilon_r \cos(\{\omega_s + \omega_D\}t + \theta_1) \quad (2.2)$$

where $\omega_s = 2\pi f_s$, $\omega_R = 2\pi f_R$ and the phase based on the scatterer distance from the phase shifts initiated within the receiver and the transducer is θ_1 (Cobbald, 1989).

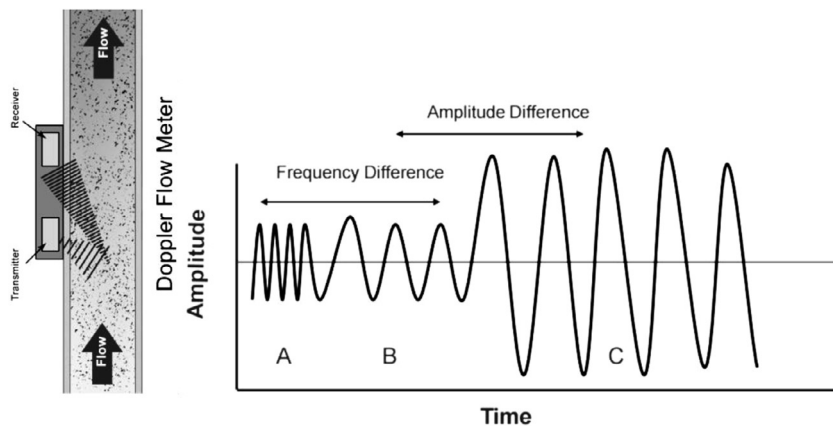


Figure 1. Principles of Ultrasonic sensor (Nnabuife et al., 2019)

Multiplying the two signals electronically will give

$$x_i(t)x_r(t) = \varepsilon_i \varepsilon_r \cos(\omega_s t) \cos([\omega_s + \omega_D]t + \theta_1) \quad (2.3)$$

$$x_i(t)x_r(t) = \frac{\varepsilon_i \varepsilon_r}{2} \{ \cos(\omega_D t + \theta_1) + \cos([2\omega_s + \omega_D]t + \theta_1) \} \quad (2.4)$$

Hence, the resulting signal is finally low-pass filtered to get rid of the $2f_s$ source frequency and leaving only the Doppler signal (Cobbold, 1989).

$$x_D(t) = \frac{\varepsilon_i \varepsilon_r}{2} \cos(\omega_D t + \theta_1) \quad (2.5)$$

However, because the received ultrasound signal has reflected ultrasound of larger amplitude than the signal backscattered from the moving scatterer, further signal processing may be required (Kuang et al., 2021). Doppler shifts at a low frequency in this form of reflected ultrasound. As a result, to eliminate this anomaly, band-pass filtering may be required (Cobbold, 1989).

The continuous wave ultrasound Doppler (CWUD) used for this study is a non-invasive flowmeter made by United Automation Ltd, which is located in Southport, England. The CWUD is appropriate for measuring ultrasonic reflecting fluid in any flow. It calculates frequency changes, analyses ultrasonic data, and estimates flow velocity. The CWUD estimates the frequency shift of signals reflected by discontinuities or scatterers in the moving fluid, such as bubbles (Nnabuife et al., 2019). To minimize air cavities trapping between the sensor and the conduit surface, a glycerin gel was used to provide a sufficient bonding between the exterior conduit surface and the sensor. The CWUD contains two independent crystal transducers integrated into a single probe that sends and receives ultrasonic signals at 500 kHz continuously (Nnabuife et al., 2020).

The CWUD utilized in this work contains two piezoelectric crystal components integrated into a single transducer. The transducer is continuously energized by the meter's electronic circuit; one of the transducers produces an ultrasonic signal, while the other receiving transducer gives the output signals (Cobbold, 1989). The flowmeter electronics then collect and amplify the incoming output signals. The processed output signal is the Doppler frequency shift signal, which was collected using a data acquisition card (NI-PCI-6040E) and a LabVIEW application that regulated the 10 kHz sampling frequency for every 0.1s for each dataset (Kremkau, 1975).

3. Experimental Setup

3.1. The Two-phase Flow Test Loop

The experiment was conducted on a 2-inch multiphase flow S-shape riser at Cranfield University's oil and gas facility. A schematic is shown in Figure 2. A clamp-on non-invasive Doppler ultrasonic transducer with

a $\pm 10V$ excitation voltage and a frequency of 500 kHz was connected to the top side of the S-shape riser. On the S-shaped riser, the ultrasonic beam incidence angle was 58 degrees with regard to the flow direction (Kuang et al., 2020). To facilitate the transfer of ultrasonic energy, a coupling substance known as the gel was placed between the pipe wall and the Doppler transducer. The Doppler ultrasonic flow meter's electronics (DFM-2, United Automation Ltd, Southport, UK) were modified to capture the voltage signals of the Doppler frequency shift for future study. The Doppler frequency shift voltage signals were acquired using the LabVIEW data acquisition system at a sampling frequency of 10 kHz and then evaluated using spectral analysis. The air utilized was provided by a bank of two parallel linked compressors. When both compressors are operating simultaneously, a maximum airflow rate of 1410m³/hr FAD at 7 barg is possible (Nnabuife et al., 2019). To decrease compressor pressure fluctuation, the air from the two compressors is collected in an 8m³ capacity receiver. Air from the receiver is routed through a bank of three filters (coarse, medium, fine) and then via a cooler, where debris and condensates are removed before the air is sent to the flow meters. A bank of two Rosemount mass probar flow meters with 12" and 1" diameters was used to measure the airflow rate. The water flow rate was provided by a water tank with a capacity of 12.5m³. Two multistage Grundfos CR90-5 pumps provided water to the flow loop. At 10 barg, the water pump has a duty of 100m³/hr. Frequency variable inverters are used to control the speed (Nnabuife et al., 2019). DeltaV is used to control the water pumps remotely. A 1" Rosemount 8742 magnetic flow meter (up to 7.36 l/s) and a 3" Foxboro CFT50 Coriolis meter (up to 30kg/s) were used to measure the water flow rate. Air and water were gravity separated after the experiment in an 11.12m³ horizontal three-phase separator. The air is discharged into the atmosphere after separation and cleaning in the three-phase separator, while the water from the three-phase separator enters its 1.6m³ coalesces, where it is further cleaned before being returned to the storage tank (Nnabuife et al., 2020). The internal diameter of the 2-inch flow loop test facility utilized in this experiment is 54.8mm, the length is 40m, and the inclination is 0°. A transparent pipe in the 2-inch flow loop test portion allows for flow regime monitoring. At the topside facility, the continuous wave ultrasonic Doppler measurement equipment was installed in the test section (Nnabuife et al., 2021).

4. Results and discussions

4.1. Flow Regime Map

Flow Regime maps are excellent tools for gaining an overview of the flow regimes that may be expected for a given set of input data. Each map, however, is not generic enough to be applicable to other data sets. It describes the geometrical distribution of a multiphase fluid passing through a conduit. This distribution is described using several

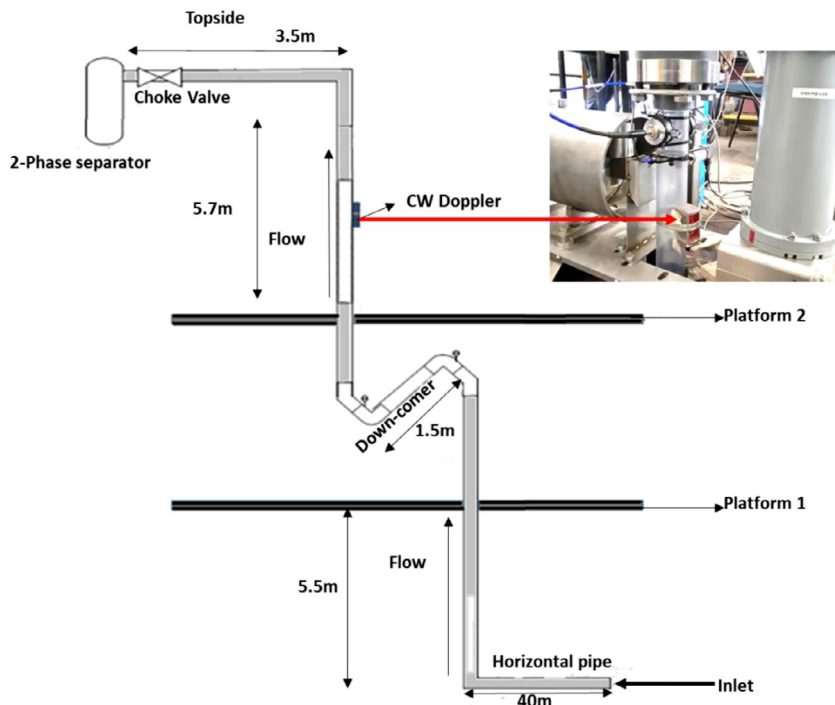


Figure 2. Schematic diagram of 2" S-shape riser

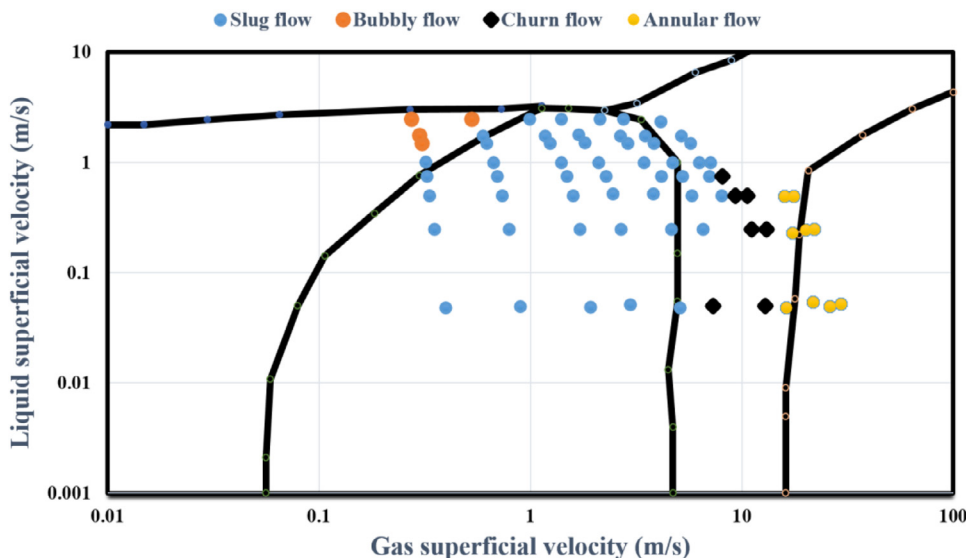


Figure 3. Experimental flow regime map for the 2" S-shaped riser (Taitel et al., 1990)

flow regimes, with the distinction between each usually qualitative and rather arbitrary (Wu et al., 2017). Figure 3 depicts the experimental flow regime map for the 2" S-shaped riser.

The flow regime map was examined to estimate the operating conditions under the severe slugging phenomenon. The selected operating points that fall into the slugging regime are gas flow rate of 10 Sm³/h and liquid flow rate of 1 kg/s with superficial velocities of 0.6941 m/s and 0.4952 m/s respectively.

4.2. Bifurcation Map

A sampling point of 1 kg/s water and 10 Sm³/h of air, which falls within the slugging flow region from Figure 3, was considered for further flow stability study. For controller design, an initial point of determining the critical point is vital, following which a controller will be developed to stabilize the system in the open-loop unstable zone. The bifurcation

map is produced by maintaining a constant flow rate and changing the valve opening. At the pivotal valve opening, the pressure sensitivity contributed by the valve to system stabilization may be calculated. Figure 4 depicts the bifurcation map for the flow condition selected from above.

Figure 4 presents the bifurcation map for the boundary condition of the 2" S-shaped riser which the system stability was obtained at a valve opening of 21%, which corresponds to a pressure of 3.8 bar. From the result of the bifurcation map, stabilizing the system at the open-loop unstable region where $u > 21\%$ will be aimed to obtain a desired stable non-oscillatory flow regime.

4.3. Controller Design

As a slug mitigation technique, an active control system operates at a higher valve opening than manual choking. Following the establishment

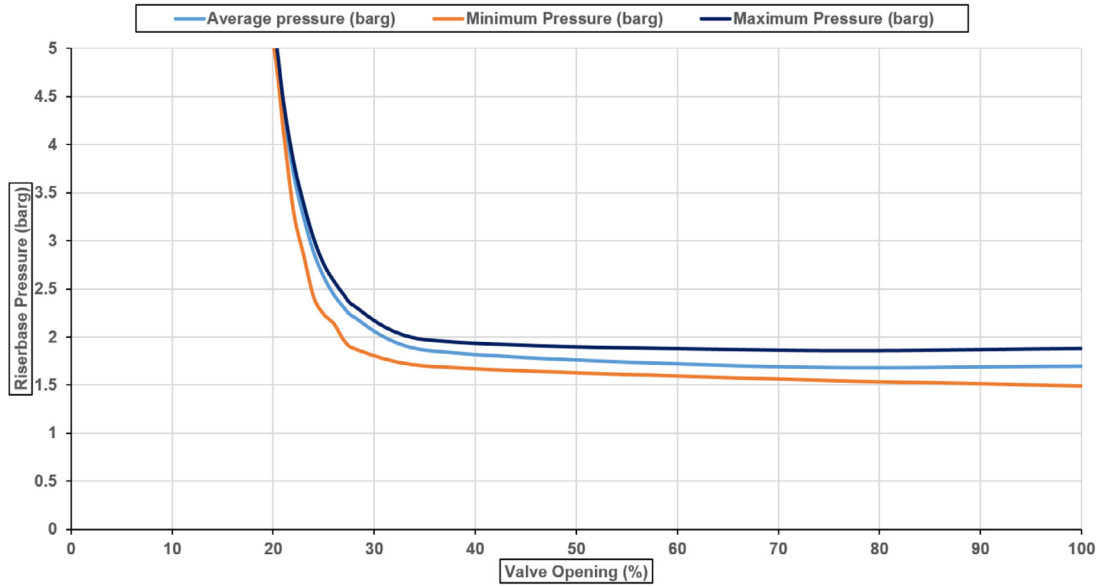
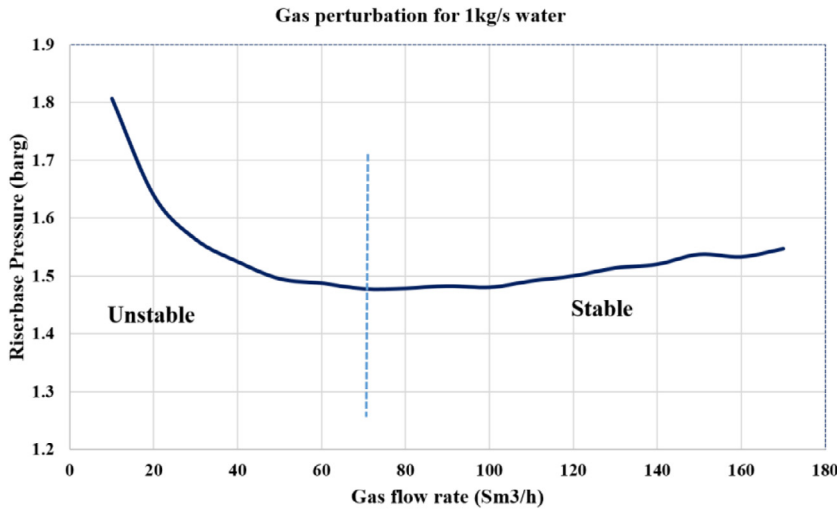
Figure 4. Bifurcation map of 1 kg/s of water and 10 Sm³/h of air

Figure 5. Gas perturbation for 1kg/s water

of the open loop system's stability point, the next goal is to control the system at a higher choke valve opening than in an open loop system.

This would act as a baseline for determining the effects of the proposed measurement on the system. The riser base pressure indicates the pipeline system throughput, whereas the pressure gradient indicates the system's stability. Stability is estimated by $DP/dQ > 0$ whereas $DP/dQ < 0$ is an unstable flow.

At a choke valve opening of 25%, the inferential slug controller (ISC) was designed to suppress the system. Tandoh et al. (Tandoh et al., 2016), described a methodology for designing controller parameters. According to (Tandoh et al., 2016), the minimum gain K of the ISC for any preferred pressure drop gradient at a specific choke valve opening could be estimated using the mathematical expression below in the quest to suppress slug flow at a higher choke valve opening.

$$\frac{d\Delta P_v}{dQ_g} = \frac{2aQ_g}{u^2} + \frac{2aQ_g^2}{u^3} K [W^T \frac{dY}{dQ_g}]$$

where a is a constant associated with valve coefficient, mixture density, and the given reference liquid flow rate; Q_g is the gas flow rate, and u is the valve opening ranging from 0 to 1; $K = du/dc$ is the controller gain to be designed, and $W^T dY/dQ_g$ is estimated from the weighted devia-

tions in measurements resulting from the perturbation of Q_g . Figure 5 depict the gas perturbation for 1kg/s of water.

Since the Inferential Slug Controller (ISC) can use any available signals from the riser system's topside, approximated velocity measurements using ultrasonic signals were used in this study. The measurement signal weights were used to estimate controller gains in a cascade setup for the ISC.

4.4. Active Controller Data Analysis

Following the establishment of the bifurcation point by controlled choking and the pressure gradient supplied by the valve, the next aim is to regulate the system response at greater valve openings. This was accomplished by adjusting the active controller based on ultrasonic data obtained at the initiation of slug flow in the pipeline-riser system. Figure 6 depicts a graphical representation of the riserbase pressure response with their equivalent valve opening utilising Doppler ultrasound velocity measurement.

Slug flow stability using velocity measured from CW Doppler was able to stabilize the flow from a valve opening of 22% open-loop unstable to 26%. Hence, this shows good control performance, having in

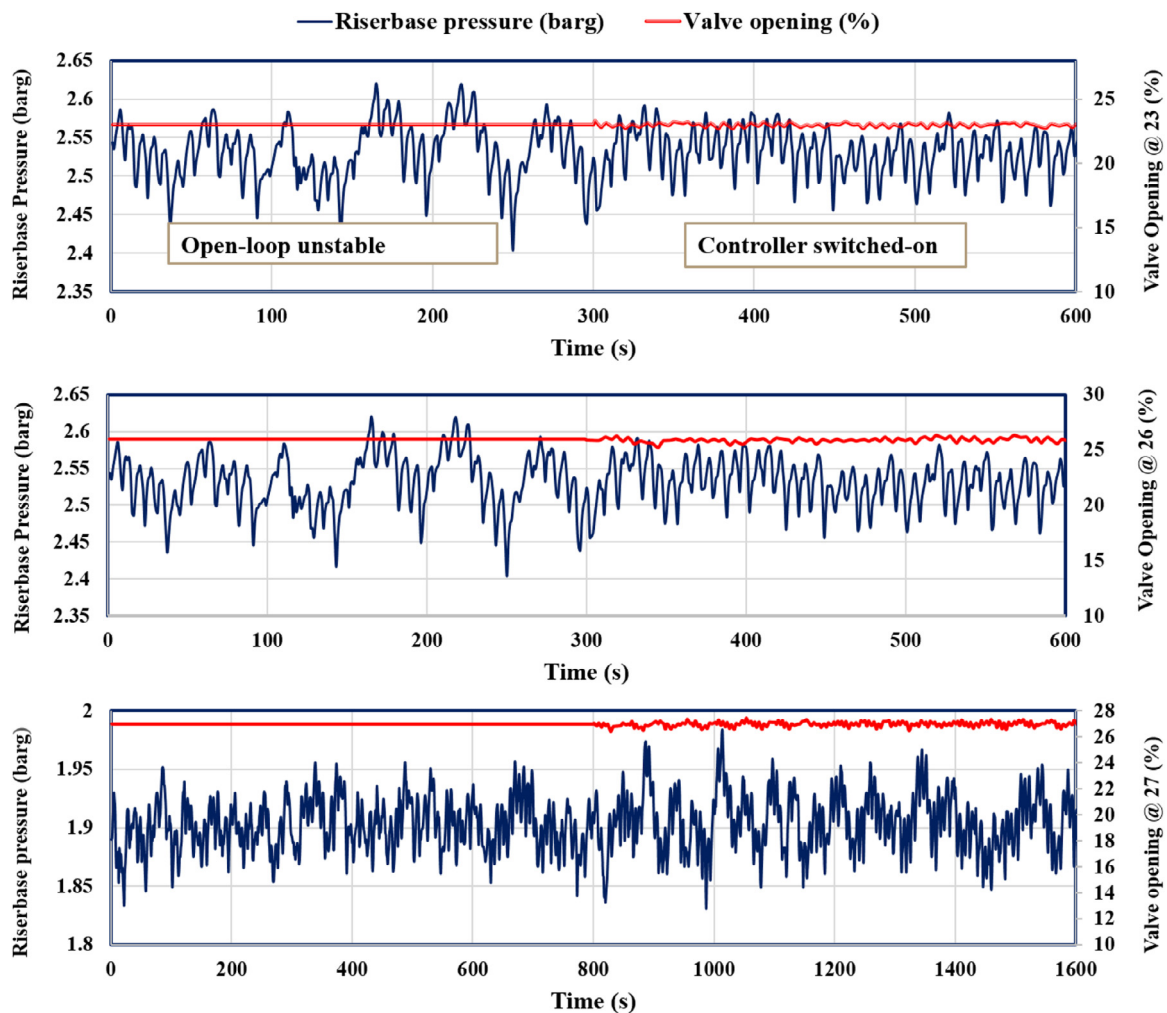


Figure 6. Riserbase pressure response with their equivalent valve opening using velocity measurement from CW Doppler ultrasound

mind that, using manual choking, the flow was stabilized at 21% valve opening.

5. Conclusion

An effort was made to control the riser slug flow using velocity measured by CW Doppler ultrasound. The results proved that velocity from CW Doppler was able to stabilise the flow from a valve opening of 22% open-loop unstable to 26%. Hence, this shows good control performance, having in mind that, using manual choking, the flow was stabilised at 21% valve opening.

The study led to the following findings:

- A novel approach to slug flow control has been described.
- When compared to manual choking, active feedback control improves slug reduction by adjusting the pressure drop across the valve.
- Also, with the assistance of a robust slugging controller, the proposed technique may yield more benefits.
- The proposed method may be able to replace the use of a Gamma densitometer, which is dangerous to human health.

References

- Havre, K., Stornes, K.O., Stray, H., 2000. Taming slug flow in pipelines. *ABB Rev* 2000 (4), 55–63.
- Payne, R.L., Huff, R.E., Ogren, W.E., 1996. Slug flow mitigation control system and method 5 (544), 672.

- Y. Cao, Inferential slug control system field trial summary, Cranfield, 2011.
- Taitel, Y., Vierkandt, S., Shoham, O., Brill, J., 1990. Severe slugging in a riser system : experiments and modeling. *Int. J. Multiph. Flow.* 16, 57–68. doi:10.1016/0301-9322(90)90037-J, https://doi.org/.
- G.F. Hewitt, D.N. Roberts, Studies of two-phase flow patterns by simultaneous X-ray and flash photography, Harwell, Berkshire, 1969. https://doi.org/a953138.pdf.
- Taitel, Y., 1986. Stability of severe slugging. *Int. J. Multiph. Flow.* 12, 203–217. doi:10.1016/0301-9322(86)90026-1, https://doi.org/.
- Barnea, D., 1987. A unified model for predicting flow-pattern transitions for the whole range of pipe inclinations. *Int. J. Multiph. Flow.* 13, 1–12. doi:10.1016/0301-9322(87)90002-4, https://doi.org/.
- Griffith, P., 1961. G.B.W. I, Two-phase slug flow. *Heat Transf* 83, 307–318.
- Pedersen, S., Durdevic, P., Yang, Z., 2017. Challenges in slug modeling and control for offshore oil and gas productions : A review study. *Int. J. Multiph. Flow.* 88, 270–284. doi:10.1016/j.ijmultiphaseflow.2016.07.018, https://doi.org/.
- Schmidt, H., Brill, Z., Beggs, J.P., 1979. Choking can eliminate severe pipeline slugging. *Oil Gas J* 12, 230–238.
- Pal, Hedne, Harald, Linga, 1990. Suppression of terrain slugging with automatic and manual riser choking. In: *Winter Annu. Meet. ASME. Dallas, Texas*, pp. 453–460.
- Courbot, A., 1996. Prevention of severe slugging in the Dunbar 16' multiphase pipeline. In: *Offshore Technol. Conf. Houston, Texas*, pp. 445–452. doi:10.4043/8196-ms https://doi.org/.
- Godhavn, J.M., Fard, M.P., Fuchs, P.H., 2005. New slug control strategies, tuning rules and experimental results. *J. Process Control.* 15, 547–557. doi:10.1016/j.procont.2004.10.003, https://doi.org/.
- Nnabuike, S.G., Tandoh, H., Whidborne, J., 2021. Slug Flow Control Using Topside Measurements : A Review. *Chem. Eng. J. Adv.*, 100204 doi:10.1016/j.cej.2021.100204, https://doi.org/doi.org/.
- Cao, Y., Lao, L., Yeung, H., 2013. Method, controller and system for controlling the slug flow of a multiphase liquid US8489244.
- Zhai, L.S., De Jin, N., Gao, Z.K., Wang, Z.Y., Li, D.M., 2013. The ultrasonic measurement of high water volume fraction in dispersed oil-in-water flows. *Chem. Eng. Sci.* 94, 271–283. doi:10.1016/j.ces.2013.02.049, https://doi.org/.

- Nnabuife, S.G., Kuang, B., Whidborne, J.F., Rana, Z., 2020. Non-Intrusive classification of gas-liquid flow regimes in an s-shaped pipeline riser using a Doppler ultrasonic sensor and deep neural networks. *Chem. Eng. J.* 403, 126401. doi:[10.1016/j.cej.2020.126401](https://doi.org/10.1016/j.cej.2020.126401), <https://doi.org/https://doi.org/>.
- Takeda, Y., 1999. Ultrasonic Doppler method for velocity profile measurement in fluid dynamics and fluid engineering. *Exp. Fluids*. 26, 177–178. doi:[10.1007/s003480050277](https://doi.org/10.1007/s003480050277), <https://doi.org/>.
- Atkinson, P., Wells, P.N., 1977. Pulse-Doppler ultrasound and its clinical application. *Yale J. Biol. Med.* 50, 367–373. <http://www.pubmedcentral.nih.gov/articlerender.fcgi?artid=2595531&tool=pmcentrez&rendertype=abstract>.
- Okamura, S., Uchida, S., Katsumata, T., Iida, K., 1989. Measurement of solids holdup in a three-phase fluidized bed by an ultrasonic technique. *Chem. Eng. Sci.* 44, 196–198. doi:[10.1016/0009-2509\(89\)85246-7](https://doi.org/10.1016/0009-2509(89)85246-7), <https://doi.org/>.
- Weinstein, E., 1982. Measurement of the differential doppler shift. *IEEE Trans. Acoust.* 30, 112–117. doi:[10.1109/TASSP.1982.1163849](https://doi.org/10.1109/TASSP.1982.1163849), <https://doi.org/>.
- Nnabuife, S.G., Pilario, K.E.S., Lao, L., Cao, Y., Shafiee, M., 2019. Identification of gas-liquid flow regimes using a non-intrusive Doppler ultrasonic sensor and virtual flow regime maps. *Flow Meas. Instrum.* 68, 101568. doi:[10.1016/j.flowmeasinst.2019.05.002](https://doi.org/10.1016/j.flowmeasinst.2019.05.002), <https://doi.org/>.
- Cobbold, R., 1989. Doppler ultrasound: Physics, instrumentation, and clinical applications. *J. Biomed. Eng.* 11, 528. doi:[10.1016/0141-5425\(89\)90051-4](https://doi.org/10.1016/0141-5425(89)90051-4), <https://doi.org/>.
- Kuang, B., Godfrey, S., Rana, Z., 2021. Pseudo-image-feature-based identification benchmark for multi-phase flow regimes. *Chem. Eng. J. Adv.* 5, 100060. doi:[10.1016/j.cej.2020.100060](https://doi.org/10.1016/j.cej.2020.100060), <https://doi.org/https://doi.org/>.
- Kremkau, F.W., 1975. Physical principles of ultrasound. *Semin. Roentgenol.* 10, 259–263. doi:[10.1016/0037-198X\(75\)90045-0](https://doi.org/10.1016/0037-198X(75)90045-0), <https://doi.org/>.
- Kuang, B., Nnabuife, S.G., Rana, Z., 2020. Pseudo-image-feature-based Identification Benchmark for Multi-phase Flow Regimes. *Chem. Eng. J. Adv.*, 100060 doi:[10.1016/j.cej.2020.100060](https://doi.org/10.1016/j.cej.2020.100060), <https://doi.org/>.
- Nnabuife, S.G., Whidborne, J., Lao, L., Cao, Y., 2019. Venturi multiphase flow measurement based active slug control. In: *ICAC 2019 - 2019 25th IEEE Int. Conf. Autom. Comput.*, Chinese Automation and Computing Society in the UK - CACSUK, Lancaster, UK, pp. 1–6. doi:[10.23919/ICAC.2019.8895212](https://doi.org/10.23919/ICAC.2019.8895212) <https://doi.org/>.
- Nnabuife, S.G., Kuang, B., Whidborne, J.F., Rana, Z.A., 2021. Development of Gas-Liquid Flow Regimes Identification Using a Noninvasive Ultrasonic Sensor, Belt-Shape Features, and Convolutional Neural Network in an S-Shaped Riser. *IEEE Trans. Cybern.* doi:[10.1109/TCYB.2021.3084860](https://doi.org/10.1109/TCYB.2021.3084860), <https://doi.org/>.
- Wu, B., Firouzi, M., Mitchell, T., Rufford, T.E., Leonardi, C., Towler, B., 2017. A critical review of flow maps for gas-liquid flows in vertical pipes and annuli. *Chem. Eng. J.* 326, 350–377. doi:[10.1016/j.cej.2017.05.135](https://doi.org/10.1016/j.cej.2017.05.135), <https://doi.org/>.
- Tandoh, H., Cao, Y., Avila, C., 2016. Stability of severe slug flow in U-shape riser. In: *22nd Int. Conf. Autom. Comput. (ICAC 2016)*, IEEE, Colchester, United Kingdom, pp. 372–377. doi:[10.1109/ICAC.2016.7604948](https://doi.org/10.1109/ICAC.2016.7604948) <https://doi.org/>.

2021-12-11

Slug flow control in an S-shape pipeline-riser system using an ultrasonic sensor

Nnabuike, Somtochukwu Godfrey

Elsevier

Nnabuike SG, Tandoh H, Whidborne J. (2022) Slug flow control in an S-shape pipeline-riser system using an ultrasonic sensor, Digital Chemical Engineering, Volume 2, Issue March, March 2022, Article number 100005

<https://doi.org/10.1016/j.dche.2021.100005>

Downloaded from Cranfield Library Services E-Repository